Available online at www.sciencedirect.com
ScienceDirect
Journal of Organometallic Chemistry 691 (2006) 4196–4203
Journal of Organometallic Chemistry
www.elsevier.com/locate/jorganchem

Synthesis, characterization and ethylene oligomerization studies of nickel complexes bearing 2-imino-1,10-phenanthrolines

Wen-Hua Sun [a,*], Shu Zhang [a], Suyun Jie [a], Wen Zhang [a], Yan Li [a], Hongwei Ma [a], Jiutong Chen [b], Katrin Wedeking [a], Roland Fröhlich [c]

[a] *Key Laboratory of Engineering Plastics and Beijing National Laboratory for Molecular Sciences, Institute of Chemistry, Chinese Academy of Sciences, Beijing 100080, China*
[b] *State Key Laboratory of Structural Chemistry, Fujian Institute of Research on the Structure of Matter, Chinese Academy of Sciences, Fuzhou 350002, China*
[c] *Organisch-Chemisches Institut der Universität Münster, Corrensstr. 40, 48149 Münster, Germany*

Received 4 May 2006; received in revised form 14 June 2006; accepted 21 June 2006
Available online 30 June 2006

Abstract

A series of nickel (II) complexes ligated by 2-imino-1,10-phenanthrolines were synthesized and characterized by elemental and spectroscopic analysis as well as by single-crystal X-ray crystallography. X-ray crystallographic analysis reveals complexes **3**, **5**, **7** and **11** as the five-coordinated distorted trigonal-bipyramidal geometry. Upon activation with Et_2AlCl, these complexes exhibited considerably high activity for ethylene oligomerization (up to 3.76×10^7 g mol^{-1}(Ni) h^{-1} for **12** with 10 equiv. of PPh_3). The ligand environment and reaction conditions significantly affect the catalytic activity of their nickel complexes.

Keywords: 2-Imino-1,10-phenanthrolinyl ligands; Nickel complexes; Ethylene oligomerization

1. Introduction

The oligomerization of ethylene is one of the major industrial processes for the production of linear α-olefins. In the past decade, homogeneous complex catalytic systems for the ethylene polymerization and oligomerization have attracted great attentions in both academic and industrial research [1]. Late-transition metal complexes have played an important role in searching the homogeneous catalytic systems due to their advantage that by carefully tuning of the ligands the corresponding catalytic products' composition can vary from lower oligomers to polymer. Among the studies of late-transition metal complexes, nickel complexes attract much interest because a nickel complex was evidentially proved as good catalyst for ethylene oligomerization in SHOP process [2]. The discovery of diimino cationic nickel complexes [3] as effective catalysts for ethylene oligomerization and polymerization resurrected the interest in designing new complexes for this purpose. In the following, Brookhart and Gibson groups individually reported 2,6-bis(imino)pyridyl metal (iron and cobalt) complexes as highly active catalysts for ethylene polymerization and oligomerization in 1998 [4]. Focusing on nickel complexes as catalysts for ethylene reactivity, they are commonly four-coordinated nickel dihalides containing bidentate ligands such as P^N [5], P^O [6], N^N [7], or N^O [8]. Intensive researches have showed the moderate to high catalytic activities for ethylene reactivity by the five-coordinated nickel halides incorporated with tridentate ligands of N^N^O [9], P^N^N [10], P^N^P [10] and N^N^N [11]. The initial idea of designing 2,9-bis(imino)-1,10-phenanthroline derivatives as N^N^N tridentate ligands for metal complexes [11] was to obtain the iron complexes as highly active catalysts. However, the iron catalysts showed very low activity for ethylene reactivity, in

* Corresponding author. Tel.: +86 10 62557955; fax: +86 10 62618239.
E-mail address: whsun@iccas.ac.cn (W.-H. Sun).

0022-328X/$ - see front matter © 2006 Elsevier B.V. All rights reserved.
doi:10.1016/j.jorganchem.2006.06.028

which the additional imino group was responsible for the problem [12]. The N^N^N nickel complexes with high catalytic activities encouraged further researches, however, the new designed tridentate N^N^N complexes exhibited low activity of ethylene dimerization (up to 15400 mol mol^{-1}(Ni) h^{-1}) [13]. On the base of considering highly active iron catalyst, we endeavoured to prepare 2-imino-1,10-phenanthroline derivatives and their iron complexes. As expected, the desired iron complexes performed high activities for ethylene reactivity [14]. Following that, the arising interest is to synthesize their nickel analogues and investigate the catalytic behavior of the nickel complexes.

The title complexes were routinely synthesized by the reaction of 2-imino-1,10-phenanthroline derivatives with nickel halides. After scanning various co-catalysts, diethylaluminium chloride (Et_2AlCl) was identified as the best co-catalyst for current nickel catalysts. The nickel catalytic system showed high catalytic activity up to 3.76×10^7 g mol^{-1}(Ni) h^{-1} of ethylene oligomerization in the presence of Ph_3P. This is one kind of the highest catalytic performance for nickel complexes in ethylene reactivity in addition to diimino nickel catalysts [3,15]. Herein we describe the synthesis and characterization of the title nickel complexes as well as their catalytic behaviors in ethylene oligomerization.

2. Results and discussion

2.1. Synthetic aspects

The ligands were efficiently synthesized according to our reported procedures [14]. Their nickel complexes were easily synthesized by reactions of $NiCl_2 \cdot 6H_2O$ with the corresponding 2-imino-1,10-phenanthroline derivatives in ethanol (Scheme 1). The mixture of $NiCl_2 \cdot 6H_2O$ with the corresponding 2-imino-1,10-phenanthroline derivatives was stirred at room temperature for 3 h, the resulting solution was concentrated and diethyl ether was then added to precipitate the product. The resulting precipitate was collected, washed with diethyl ether and dried in vacuum. All of the complexes were prepared by this method in high yields, except for complex **7** being synthesized through the reaction of the corresponding ligand with $(DME)NiBr_2$ in dichloromethane under nitrogen atmosphere. All complexes were fully characterized by IR spectra and elemental analyses, nevertheless, the unambiguous molecular structures were confirmed through the single-crystal X-ray diffraction studies of complexes **3**, **5**, **7** and **11**.

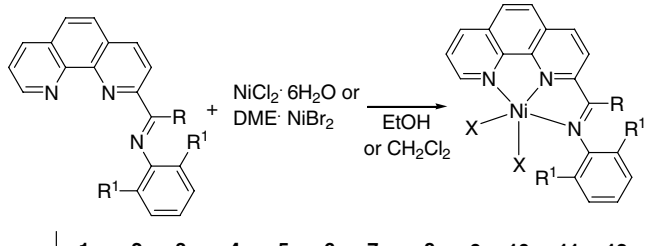

	1	2	3	4	5	6	7	8	9	10	11	12
R	H	H	H	H	Me	Me	Me	Me	Me	Ph	Ph	Ph
R^1	Me	Et	i-Pr	F	Me	Et	Et	i-Pr	F	Me	Et	i-Pr
X	Cl	Cl	Cl	Cl	Cl	Cl	Br	Cl	Cl	Cl	Cl	Cl

Scheme 1. Synthesis of complexes **1**–**12**.

2.2. Molecular structures

Crystals of complexes **3**, **5**, **7** and **11** suitable for single-crystal X-ray diffraction were obtained by re-crystallization through the slow diffusion of diethyl ether into their methanol solution, respectively. Analysis of X-ray crystallography reveals that all complexes display the distorted trigonal bipyramidal geometry, in which the nickel core is coordinated with the tridentate ligand and two halides. The nitrogen (N3) of the imino group and one nitrogen (N1) of the phenanthrolinyl group with the nickel core form an axial plane while the equatorial plane consists of one nitrogen atom (N2) and two halide atoms. Their selected bond lengths and bond angles are collected in Table 1, meanwhile their molecular structures are shown in Figs. 1,3,6,7, individually.

In complex **3**, the data show the nickel atom deviates by 0.0015 Å from the equatorial plane. The two nitrogen

Table 1
Selected bond lengths (Å) and bond angles (°) for **3**, **5**, **7** and **11**

	3	5	7	11
Bond lengths				
Ni–N(1)	2.168(2)	2.157(3)	2.160(2)	2.156(2)
Ni–N(2)	1.9938(2)	1.987(3)	1.988(2)	1.999(2)
Ni–N(3)	2.2436(2)	2.194(3)	2.181(2)	2.225(2)
Ni–Cl(1)	2.2307(7)	2.2522(1)		2.2552(8)
Ni–Br(1)			2.4005(4)	
Ni–Cl(2)	2.2784(8)	2.2863(1)		2.2707(8)
Ni–Br(2)			2.4321(4)	
N(1)–C(1)	1.327(4)	1.321(5)	1.320(3)	1.323(4)
N(1)–C(11)	1.354(3)	1.364(4)	1.371(3)	1.357(3)
N(2)–C(10)	1.329(3)	1.326(4)	1.320(3)	1.334(3)
N(2)–C(12)	1.346(3)	1.348(4)	1.338(3)	1.343(3)
N(3)–C(13)	1.272(3)	1.284(4)	1.288(3)	1.294(3)
Bond angles				
N(2)–Ni–N(1)	77.84(8)	78.19(12)	78.15(9)	78.21(9)
N(2)–Ni–N(3)	75.11(7)	75.03(12)	75.58(8)	74.88(9)
N(1)–Ni–N(3)	151.40(8)	151.99(11)	152.37(8)	152.45(8)
N(2)–Ni–Cl(1)	146.23(6)	153.12(8)		142.02(7)
N(2)–Ni–Br(1)			153.17(6)	
N(1)–Ni–Cl(1)	99.15(6)	97.69(9)		97.64(6)
N(1)–Ni–Br(2)			91.92(6)	
N(3)–Ni–Cl(1)	98.15(5)	102.44(9)		99.88(6)
N(3)–Ni–Br(2)			99.37(5)	
N(2)–Ni–Cl(2)	96.74(6)	96.18(8)		104.31(6)
N(2)–Ni–Br(2)			96.49(6)	
N(1)–Ni–Cl(2)	92.89(6)	92.98(8)		93.62(6)
N(1)–Ni–Br(1)			97.76(6)	
N(3)–Ni–Cl(2)	99.29(5)	97.86(8)		98.57(6)
N(3)–Ni–Br(1)			101.77(6)	
Cl(1)–Ni–Cl(2)	117.03(3)	110.62(4)		113.65(3)
Br(2)–Ni–Br(1)			110.210(2)	

atoms (N1 and N3) occupy the axial coordination sites with the bond angle of 151.40(8)° for N(1)–Ni–N(3). The equatorial plane and the axial plane form a dihedral angle of 87.5°. Analysis of the packing diagram of complex **3** (Fig. 2) shows the distance of H2A···Cl2 is 2.804 Å and shorter than the anticipated van der Waals radii (3.0 Å) of H and Cl atoms indicating hydrogen bond is formed between them in the solid state. The intermolecular hydrogen-chloride bonding links the molecules to form the zigzag polymer chains (Fig. 2).

Similar to the structure of complex **3**, the axial positions are occupied by nickel with two nitrogen atoms N1 and N3 [N(1)–Ni–N(3) = 151.99(11)°] while the equatorial plane is constructed with N2 and two chlorides in the structure of complex **5** (see Fig. 3). The deviation of the nickel atom from the equatorial plane is 0.0322 Å. The dihedral angle between its equatorial and axial planes is 89.4°. The C_6 central ring of phenanthroline of one nickel complex interacts in a ''face-to-face'' fashion with another C_6 central ring of phenanthroline in the adjacent nickel moiety with the relevant plane-to-plane distance of 3.201 Å, however, its center-to-center distance is 3.625 Å (Fig. 4). In addition, there exists a certain C–H···Cl hydrogen bond interactions between two molecules with the bonding distance C(8)–H(8B)···Cl(2) of 2.634 Å. Two molecules form a dimmer, bridged by hydrogen bonds, and the dimers extend to form a parallel supramolecular architecture through π–π interaction, which link small metallo-supramolecular blocks into infinite one-dimensional chain polymer (Fig. 5).

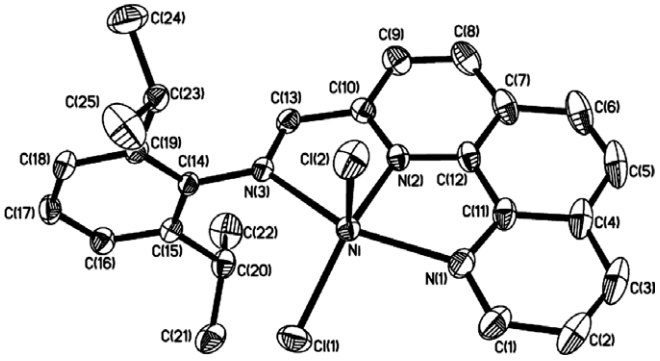

Fig. 1. Crystal structure of complex **3**. Hydrogen atoms were omitted for clarity.

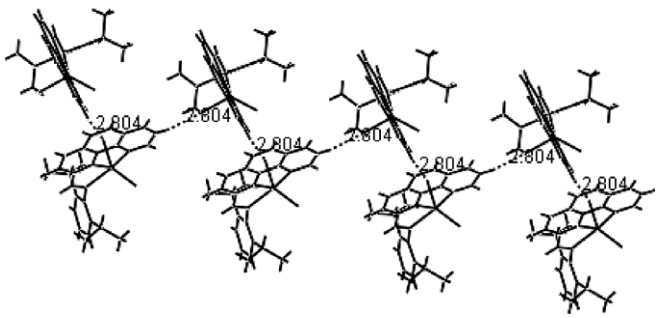

Fig. 2. Part of the zigzag polymer chains present in the structure of **3**.

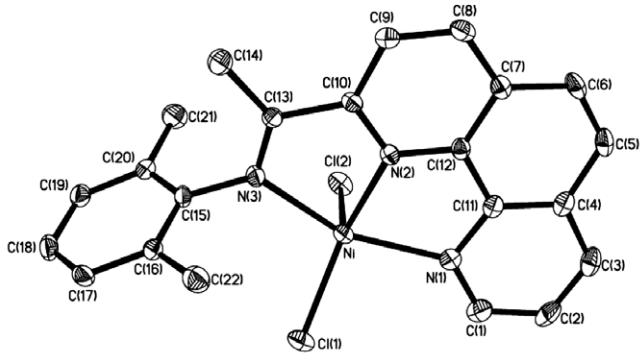

Fig. 3. Crystal structure of complex **5**. Hydrogen atoms were omitted for clarity.

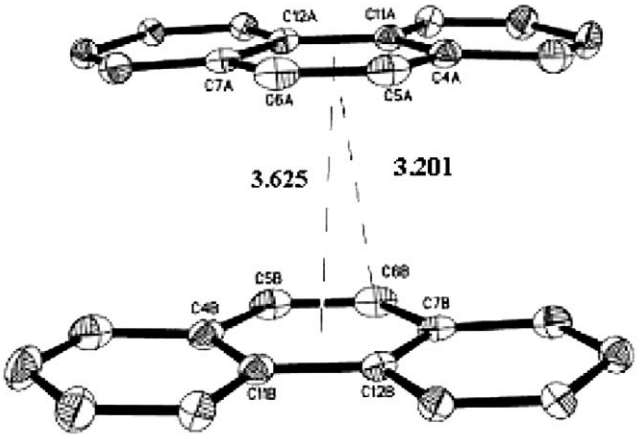

Fig. 4. π–π Stacking between the molecules.

The molecular structure of complex **7** is shown in Fig. 6. In the molecule, the equatorial plane contains N(2), Br(1), Br(2) atoms while the other two atoms N(1) and N(3) occupy the axial positions. The angle of N1–Ni–N3 is 152.37(8)° and the nickel atom locates 0.0414 Å above the equatorial plane toward N3. The dihedral angle of the equatorial and axial planes is 88.3°. The solid structure of complex **7** showed similar structural feathers of intermolecular hydrogen bond observed in complex **3**, and of intermolecular ''face-to-face'' fashion π–π interaction of the adjacent phenanthroline rings appeared in complex **5**.

In complex **11**, the axial positions are occupied by nickel with two nitrogen atoms N1 and N3 [N(1)–Ni–N(3) = 152.45(8)°], and the nickel atom locates 0.0172 Å above the equatorial plane toward N3. The dihedral of the equatorial plane and the axial plane is 88.9°. Similar weak interaction of hydrogen bonds is also observed in this complex.

Compared with 2,9-diformyl-1,10-phenanthroline-bis (2,6-diisopropylanil)nickel (II) complex [11], the title complexes can also be described as a distorted trigonal bipyra-

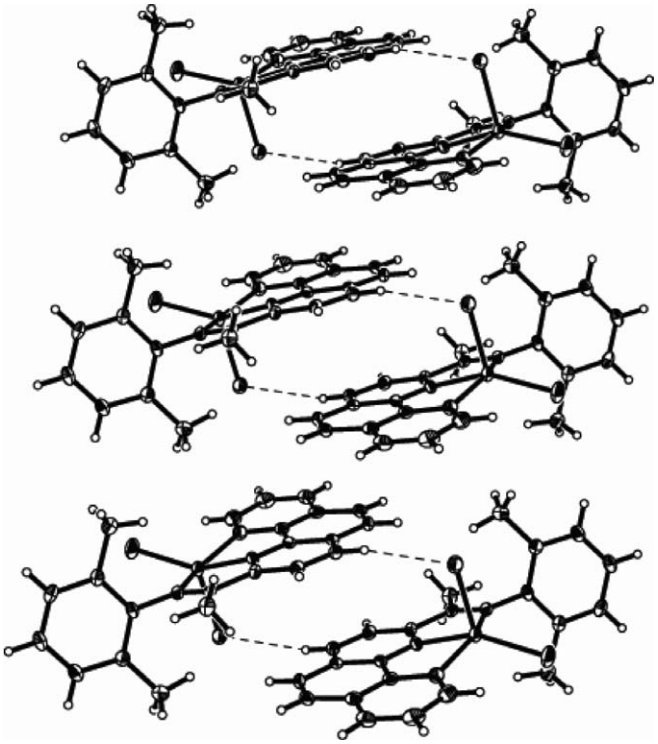

Fig. 5. Side view of polymer chains present in the structure of **5**.

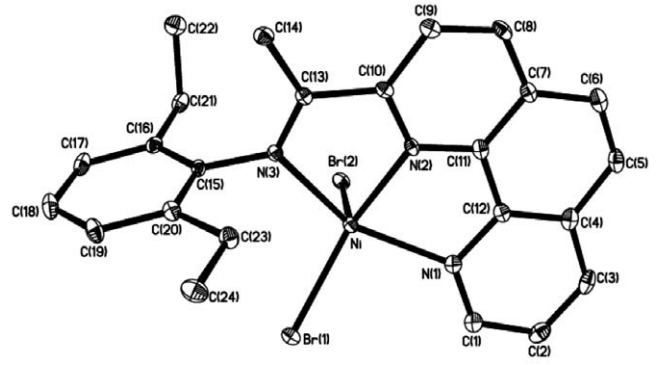

Fig. 6. Crystal structure of complex **7**. Hydrogen atoms were omitted for clarity.

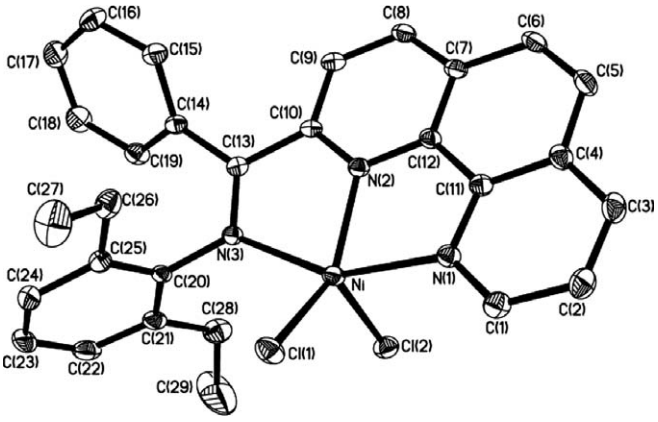

Fig. 7. Crystal structure of complex **11**. Hydrogen atoms were omitted for clarity.

midal. The two axial Ni–N bond (2.168 and 2.244 Å for complex **3**, 2.157 and 2.194 Å for complex **5**, 2.160 and 2.181 Å for complex **7**, 2.156 and 2.225 Å for complex **11**) are longer than that of Ni–N(2) of the equatorial plane (1.994 Å for complex **3**, 1.987 Å for complex **5**, 1.988 Å for complex **7**, 1.999 Å for complex **11**). In nickel complexes ligated by 2,9-diimino-1,10-phenanthroline ligands [11], the ring atoms of the 1,10-phenanthroline ligand and C(13), N(1), C(26), N(4) of the imino groups as well as the Ni(1) atom form an almost perfect plane. However, the co-plane phenomena were not observed in the title complexes. The nickel atoms deviate from the phenanthroline plane in a longer distance (0.2572 Å for complex **3**, 0.2969 Å for complex **5**, 0.3346 Å for complex **7**, 0.2326 Å for complex **11**).

2.3. Ethylene oligomerization

The nickel (II) complexes **1**–**12** were systematically investigated for the ethylene oligomerization. Compared with the nickel (II) complexes incorporating 2,9-diimino-1,10-phenanthrolines [11], which showed good activity (10^6 g mol^{-1}(Ni) h^{-1}) with MAO as co-catalyst, the title nickel complexes ligated by 2-imino-1,10-phenanthrolines only reached low activity (about 10^4 g mol^{-1}(Ni) h^{-1}) in the presence of MAO even increasing ethylene pressure. After various alkylaluminums (and their oxides) as co-catalysts were scanned in activating the title nickel complexes for ethylene reactivity at ambient pressure of ethylene, the catalytic system using diethylaluminium chloride (Et_2AlCl) had better response with the observed catalytic activities in the order of 10^4 g mol^{-1}(Ni) h^{-1}. With elevated ethylene pressure, the higher catalytic activity is obtained upon treatment with Et_2AlCl. Therefore all further investigation will use Et_2AlCl as the activator. In accordance with the oligomers of C4 and C6 produced, the catalytic reaction mixture was hydrolyzed with HCl acid in ice-water bath and analyzed by GC in order to prevent the loss of more volatile C4.

2.3.1. Effects of reaction parameters on catalytic activity

As the ethylene reactivity considered, the reaction parameters including reaction temperature, the ratio of Et_2AlCl to nickel complex and the pressure of ethylene affect their catalytic activities. Due to the lower activity at ambient pressure of ethylene, ethylene oligomerization at elevated pressures was carried out and the results were collected in Table 2.

The influence of the ethylene pressure and reaction temperature on ethylene oligomerization were investigated in detail with complex **8**, which showed low activity (2.8×10^4 g mol^{-1}(Ni) h^{-1}) at 1 atm ethylene pressure. A sharp increase in the activity was observed when the ethylene pressure was increased (entries 1–3 in Table 2). The elevation of the reaction temperature resulted in a significant decline in the activity (entries 3, 6 and 7 in Table 2), which may be attributed to the decomposition of the catalysts and lower ethylene solubility at higher temperature.

Table 2
Ethylene oligomerization with **1**–**12**/Et_2AlCl

Entry	Cat.	Al/Ni	*P* (atm)	*T* (°C)	Activity (g mol^{-1}(Ni) h^{-1})	Oligomer distribution (%)	
						C4	C6
1	**8**	200	10	20	2.10×10^5	100	0
2	**8**	200	20	20	2.49×10^5	95.2	4.8
3	**8**	200	30	20	7.11×10^5	91.0	9.0
4	**8**	100	30	20	5.78×10^4	100	0
5	**8**	300	30	20	1.47×10^5	85.4	14.6
6	**8**	200	30	30	1.86×10^5	90.0	10.0
7	**8**	200	30	40	1.58×10^5	87.6	12.4
8	**1**	200	30	20	4.47×10^5	91.4	8.6
9	**2**	200	30	20	3.25×10^5	89.8	10.2
10	**3**	200	30	20	4.72×10^5	91.1	8.9
11	**4**	200	30	20	1.74×10^5	85.7	14.3
12	**5**	200	30	20	1.64×10^5	88.9	11.1
13	**6**	200	30	20	2.60×10^5	88.6	11.4
14	**7**	200	30	20	2.73×10^5	88.8	11.2
15	**9**	200	30	20	1.66×10^5	84.9	15.1
16	**10**	200	30	20	1.72×10^5	88.0	12.0
17	**11**	200	30	20	2.83×10^5	89.9	10.1
18	**12**	200	30	20	1.36×10^6	93.8	6.2

Conditions. 10 μmol Ni Cat.; 30 min; in 100 ml toluene.

The effect of Al/Ni molar ratio on ethylene oligomerization were also investigated with complex **8**. With Al/Ni ratio of 200, the catalytic activity was peaked at 7.11×10^5 g mol^{-1}(Ni) h^{-1} (entries 3–5 in Table 2), however, the higher ratio of Al/Ni did not result in higher activity.

Ethylene oligomerization with complexes **1**–**12** were studied under 30 atm of ethylene pressure. The variation of the R substituent on the imino-C of ligands, 2-(ArN=CR)-1,10-phen, resulted in changes of the catalytic performance. Comparing the complexes ligated by the methyl-ketimine (R = Me), phenyl-ketimine (R = Ph) with aldimine (R = H) containing the 2,6-diisopropylphenyl group on the imino nitrogen, both **8** and **12** (entries 3 and 18 in Table 2) showed much better catalytic activity than **3** (entry 10 in Table 2). Furthermore the R substituent had different influences on methyl or phenyl-ketimine and aldimine analogues. For methyl-ketimine and phenyl-ketimine complexes, it was observed that an increase in steric hindrance of the R^1 group led to an enhanced activity, but no significant effect was noticed for aldimine complexes. The electronic effect of the substitution pattern of the phenyl ring connected with the imine nitrogen atom is not significant. The halide anion linked to the nickel center had no obvious influence on the catalytic activity (Table 2, entry 13 vs. entry 14).

2.3.2. Effects of PPh_3 as the auxiliary ligand on catalyst activity

Previous studies on nickel-based catalysts have demonstrated that incorporating PPh_3 into catalytic systems leads to higher activity and longer catalyst lifetime [8b,8f,16]. Therefore, the oligomerization reaction with **8**/Et_2AlCl was carried out with changing the equivalent amount of PPh_3, the ethylene oligomerization activities were observed as 2.8×10^4 (without PPh_3), 1.4×10^5 (2 equiv. of PPh_3), 4.7×10^5 (5 equiv. of PPh_3), 5.8×10^5 (10 equiv. of PPh_3), 6.4×10^5 (15 equiv. of PPh_3) g mol^{-1}(Ni) h^{-1}, which suggests the increasing amount of PPh_3 leads to an enhancement of the ethylene oligomerization activity. Therefore all catalytic precursors were fully studied in the presence of 10 equiv. of PPh_3, and their results were collected in Table 3. In our previous work [8f,9], the potential catalytic intermediates incorporating PPh_3 were observed. The stoichiometric amount of PPh_3 to Ni did not make sense of improving catalytic activity, however more equivalents of PPh_3 to Ni were necessary for their higher catalytic activity of ethylene oligomerization, the plausible role of PPh_3 will be association and dissociation with nickel core to activate and protect the active sites.

In the presence of 10 equiv. of PPh_3, complex **8** showed good activity in the Al/Ni molar ratio of 200–500 (entries 8, 13–15 in Table 3) at ambient pressure, and the optimum data was observed at Al/Ni molar ratio of 300 with the activity peaked at 8.36×10^5 g mol^{-1}(Ni) h^{-1}. Accordingly further investigations were carried out in the presence of 10 equiv. of PPh_3 with the ratio 300 of Al/Ni. The result showed no significant effect of the R and R^1 groups for the oligomerization activity. However, the steric and electronic effects of the aryl ring on the oligomer distribution are remarkable. Increasing the bulk on the aryl ring of the complex led to an enhancement of C6 (entries 1–3, 5–6, 8 and 10–12 in Table 3). The complexes containing electron-withdrawing halogen groups show better selectivity

Table 3
Ethylene oligomerization with **1**–**12**/Et_2AlCl and 10 equiv. of PPh_3

Entry	Cat.	Al/Ni	*P* (atm)	*T* (°C)	Activity (g mol^{-1}(Ni) h^{-1})	Oligomer distribution (%)	
						C_4	C_6
1[a]	**1**	300	1	20	6.55×10^5	73.5	26.5
2[a]	**2**	300	1	20	8.24×10^5	60.6	39.4
3[a]	**3**	300	1	20	8.70×10^5	54.4	45.6
4[a]	**4**	300	1	20	9.83×10^5	61.6	38.4
5[a]	**5**	300	1	20	6.82×10^5	94.0	6.0
6[a]	**6**	300	1	20	7.74×10^5	85.9	14.1
7[a]	**7**	300	1	20	7.04×10^5	82.3	17.7
8[a]	**8**	300	1	20	8.36×10^5	78.2	21.8
9[a]	**9**	300	1	20	1.00×10^6	53.3	46.7
10[a]	**10**	300	1	20	8.17×10^5	93.1	6.9
11[a]	**11**	300	1	20	8.60×10^5	71.3	28.7
12[a]	**12**	300	1	20	8.44×10^5	70.1	29.9
13[a]	**8**	200	1	20	5.80×10^5	79.9	20.1
14[a]	**8**	400	1	20	5.81×10^5	75.2	24.8
15[a]	**8**	500	1	20	4.00×10^5	100	0
16[b]	**5**	300	30	40	1.06×10^7	86.8	13.2
17[b]	**8**	300	30	40	3.13×10^7	87.8	12.2
18[b]	**9**	300	30	40	3.17×10^7	83.0	17.0
19[b]	**12**	300	30	40	3.76×10^7	83.1	16.9

[a] 5 μmol complex in 30 ml toluene within 30 min.
[b] 10 μmol complex in 100 ml toluene within 60 min.

for C6 (entries 4 and 9 in Table 3). In addition, some catalyst precursors were investigated at 30 atm of ethylene pressure, and their catalytic activities were sharply increased up to a very high level with the order of 10^7 g mol^{-1}(Ni) h^{-1} (entries 16–19 in Table 3), which were only observed within diimino nickel catalysts [3,15].

3. Conclusions

A series of nickel (II) complexes bearing 2-imino-1,10-phenanthrolinyl ligands have been synthesized and fully characterized. Upon treatment with Et_2AlCl, these nickel (II) complexes showed moderate activities up to 1.36×10^6 g mol^{-1}(Ni) h^{-1} for ethylene oligomerization which is higher than the reported N^N^N nickel complex [11]. Both the R on the imino-C and the substituents on the N-aryl rings had an obvious influence on the catalytic activity and distribution of oligomers due to their different steric and electronic properties. In addition, the ethylene oligomerization activities increase up to 3.76×10^7 g mol^{-1}(Ni) h^{-1} when additional PPh_3 is employed as auxiliary ligand.

4. Experimental

4.1. General

All moisture-sensitive manipulations were carried out under an atmosphere of nitrogen using standard Schlenk techniques. Solvents were refluxed over an appropriate drying agent and distilled. Elemental analyses were performed on a Flash EA 1112 microanalyzer. The IR spectra were obtained as KBr pellets on a Bruker DMX-300 spectrometer. GC analysis were performed with a Carlo Erba Strumentazione gas chromatograph equipped with a flame ionization detector and a 30 m (0.2 mm i.d., 0.25 μm film thickness) DM-1 silica capillary column. Et_2AlCl (1.90 mol l^{-1}) solution in hexane was purchased from Acros Chemicals. All other chemicals were used commercially without further purification unless stated otherwise.

4.2. Synthesis of complexes 1–12

General procedure. A solution of $NiCl_2 \cdot 6H_2O$ in ethanol or (DME) $NiBr_2$ in dichloromethane was added dropwise to a solution of the ligand in ethanol (or dichloromethane). Immediately the color of the solution changed and some precipitate formed. The reaction mixture was stirred at room temperature for 3 h then diluted with diethyl ether. The resulting precipitate was collected, washed with diethyl ether and dried in vacuum. All of the complexes were prepared in high yield in this manner.

4.2.1. 2-Formyl-1,10-phenanthroline(2,6-dimethylanil)$NiCl_2$ (1)

Obtained as orange powder in 77% yield. Anal. Calc. for $C_{21}H_{17}Cl_2NiN_3 \cdot C_2H_6O$ (487.05): C, 56.72; H, 4.76; N, 8.63. Found: C, 56.44; H, 4.60; N, 8.47%. FT-IR (KBr disc, cm^{-1}): 3062, 1609, 1511, 1408, 1185, 863, 778.

4.2.2. 2-Formyl-1,10-phenanthroline(2,6-diethylanil)$NiCl_2$ (2)

Obtained as orange powder in 72% yield. Anal. Calc. for $C_{25}H_{25}Cl_2NiN_3$ (469.03): C, 58.90; H, 4.51; N, 8.96. Found: C, 58.55; H, 4.56; N, 8.72%. FT-IR (KBr disc, cm^{-1}): 2966, 1608, 1512, 1451, 1409, 866.

4.2.3. 2-Formyl-1,10-phenanthroline(2,6-diisopropylanil)$NiCl_2$ (3)

Obtained as orange powder in 83% yield. Anal. Calc. for $C_{25}H_{25}Cl_2NiN_3$ (497.09): C, 60.41; H, 5.07; N, 8.45. Found: C, 60.22; H, 5.16; N, 8.17%. FT-IR (KBr disc, cm^{-1}): 2965, 1605, 1514, 1465, 1411, 850, 766.

4.2.4. 2-Formyl-1,10-phenanthroline(2,6-difluoroanil)$NiCl_2$ (4)

Obtained as orange powder in 42% yield. Anal. Calc. for $C_{19}H_{11}Cl_2F_2NiN_3$ (448.91): C, 50.84; H, 2.47; N, 9.36. Found: C, 51.08; H, 2.76; N, 9.06%. FT-IR (KBr disc, cm^{-1}): 3018, 1612, 1513, 1471, 1409, 864, 789.

4.2.5. 2-Acetyl-1,10-phenanthroline(2,6-dimethylanil)$NiCl_2$ (5)

Obtained as orange powder in 81% yield. Anal. Calc. for $C_{22}H_{19}Cl_2NiN_3$ (455.01): C, 58.07; H, 4.21; N, 9.24. Found: C, 57.75; H, 4.22; N, 8.92%. FT-IR (KBr disc, cm^{-1}): 3050, 1612, 1511, 1408, 1288, 1212, 865, 772.

4.2.6. 2-Acetyl-1,10-phenanthroline(2,6-diethylanil)$NiCl_2$ (6)

Obtained as orange powder in 65% yield. Anal. Calc. for $C_{24}H_{23}Cl_2NiN_3$ (483.06): C, 59.67; H, 4.80; N, 8.70. Found: C,59.64; H, 4.82; N, 8.53%. FT-IR (KBr disc, cm^{-1}): 2964, 1609, 1512, 1409, 1287, 874, 787.

4.2.7. 2-Acetyl-1,10-phenanthroline(2,6-diethylanil)$NiBr_2$ (7)

Obtained as orange powder in 87% yield. Anal. Calc. for $C_{24}H_{22}Br_2NiN_3$ (571.96): C, 50.40; H, 4.05; N, 7.35. Found: C, 50.12; H, 4.17; N, 7.10%. FT-IR (KBr disc, cm^{-1}): 2976, 1608, 1416, 1286, 863, 787.

4.2.8. 2-Acetyl-1,10-phenanthroline(2,6-diisopropylanil)$NiCl_2$ (8)

Obtained as orange powder in 90% yield. Anal. Calc. for $C_{26}H_{27}Cl_3NiN_3$ (511.11): C, 61.10; H, 5.32; N, 8.22. Found: C, 60.91; H, 5.44; N, 7.88%. FT-IR (KBr disc, cm^{-1}): 2967, 1608, 1411, 1288, 850, 790.

4.2.9. 2-Acetyl-1,10-phenanthroline(2,6-difluoroanil)$NiCl_2$ (9)

Obtained as orange powder in 83% yield. Anal. Calc. for $C_{20}H_{13}Cl_2F_2NiN_3$ (462.93): C, 51.89; H, 2.83; N, 9.08.

Found: C, 51.88; H, 3.02; N, 9.01.%. FT-IR (KBr disc, cm^{-1}): 2967, 1612, 1472, 1281, 859, 778.

4.2.10. 2-Benzoyl-1,10-phenanthroline(2,6-dimethylanil)$NiCl_2$ (**10**)

Obtained as orange powder in 62% yield. Anal. Calc. for $C_{27}H_{21}Cl_2NiN_3$ (517.08): C, 62.72; H, 4.09; N, 8.13. Found: C, 62.76; H, 3.75; N, 8.34%. FT-IR (KBr disc, cm^{-1}): 3067, 1604, 1511, 1440, 1409, 1288, 860, 768, 703.

4.2.11. 2-Benzoyl-1,10-phenanthroline(2,6-diethylanil)$NiCl_2$ (**11**)

Obtained as orange powder in 62% yield. Anal. Calc. for $C_{29}H_{25}Cl_2NiN_3$ (545.13): C, 63.90; H, 4.62; N, 7.71. Found: C, 63.89; H, 4.89; N, 7.31%. FT-IR (KBr disc, cm^{-1}): 2961, 1607, 1511, 1441, 1406, 867, 787, 701.

4.2.12. 2-Benzoyl-1,10-phenanthroline(2,6-diisopropylanil)$NiCl_2$ (**12**)

Obtained as orange powder in 85% yield. Anal. Calc. for $C_{31}H_{29}Cl_2NiN_3$ (573.18): C, 64.96; H, 5.10; N, 7.33. Found: C, 65.13; H, 5.27; N, 7.01%. FT-IR (KBr disc, cm^{-1}): 2965, 1605, 1509, 1440, 1405, 998, 863, 782, 701.

4.3. X-ray crystal structure determination of **3**, **5**, **7**, and **11**

Intensity data for complexes **3** and **7** were collected on a Brucker SMART 1000 CCD diffractometer with graphite-monochromated Mo Kα radiation ($\lambda = 0.71073$ Å). Single-crystal X-ray diffraction studies for complex **5** were carried out on a Rigaku RAXIS Rapid IP diffractometer with graphite-monochromated Mo Kα radiation ($\lambda = 0.71073$ Å). The data set for complex **11** was collected with a Nonius Kappa CCD diffractometer, equipped with a Nonius FR591 rotating anode generator. Unit cell dimensions were obtained with least-squares refinements. Intensities were corrected for Lorentz and polarization effects and empirical absorption. The structures were solved by direct methods, and refined by full-matrix least-square on F^2. Each hydrogen atom was placed in a calculated position, and refined using a riding model. All non-hydrogen atoms were refined anisotropically. Structure solution and refinement were performed using SHELXL-97 package [17]. Crystal date and processing parameters were summarized in Table 4.

Table 4
Crystal date and structure refinement for **3**, **5**, **7** and **11**

	3	**5**	**7**	**11**
Empirical formula	$C_{25}H_{25}Cl_2N_3Ni$	$C_{22}H_{19}Cl_2N_3Ni$	$C_{24}H_{23}Br_2N_3Ni$	$C_{29}H_{25}Cl_2N_3Ni$
Formula weight	497.09	455.01	571.98	545.13
Crystal color	Red	Red	Red	Red
Temperature (K)	293(2)	293(2)	130(2)	198(2)
Wavelength (Å)	0.71073	0.71073	0.71073	0.71073
Crystal system	Orthorhombic	Monoclinic	Monoclinic	Triclinic
Space group	*Pbca*	*P*2(1)/*c*	*P*2(1)/*c*	$P\bar{1}$
a (Å)	14.7112(3)	7.9214(16)	8.1478(4)	8.6570(10)
b (Å)	15.98010(10)	18.777(2)	19.7762(10)	8.7780(10)
c (Å)	19.7539(4)	13.261(3)	13.5317(7)	17.1590(10)
α (°)	90	90	90	80.990(10)
β (°)	90	102.77(3)	99.358(2)	89.200(10)
γ (°)	90	90	90	73.750(10)
Volume ($Å^3$)	4643.87(14)	1923.7(6)	2151.38(19)	1235.8(2)
Z	8	4	4	2
D_{calc} ($Mg\ m^{-3}$)	1.422	1.571	1.766	1.465
μ (mm^{-1})	1.083	1.300	4.633	1.025
F(000)	2064	936	1144	564
Crystal size (mm)	$0.52 \times 0.50 \times 0.18$	$0.262 \times 0.172 \times 0.033$	$0.20 \times 0.20 \times 0.13$	$0.30 \times 0.15 \times 0.15$
θ range (°)	2.06–25.08	2.17–27.43	3.05–27.48	2.40–28.26
Limiting indices	$-17 \leqslant h \leqslant 17$, $-15 \leqslant k \leqslant 18$, $-23 \leqslant l \leqslant 22$	$0 \leqslant h \leqslant 10$, $0 \leqslant k \leqslant 24$, $-17 \leqslant l \leqslant 16$	$-10 \leqslant h \leqslant 10$, $-25 \leqslant k \leqslant 22$, $-14 \leqslant l \leqslant 17$	$0 \leqslant h \leqslant 11$, $-10 \leqslant k \leqslant 11$, $-22 \leqslant l \leqslant 22$
Reflections collected	17435	4310	16477	11766
Unique reflections	4067	4310	4923	6001
Completeness to θ (%)	98.7 ($\theta = 25.08$)	98.4 ($\theta = 27.43$)	99.8 ($\theta = 27.48$)	98.1 ($\theta = 28.26$)
Absorption correction	Empirical	Empirical	Semi-empirical	Empirical
Data/restraints/parameters	4067/0/280	4310/0/253	4923/0/271	6001/0/318
Goodness-of-fit on F^2	1.055	0.814	1.045	1.014
Final *R* indices [$I > 2\sigma(I)$]	$R_1 = 0.0330$, $wR_2 = 0.0791$	$R_1 = 0.0467$, $wR_2 = 0.0751$	$R_1 = 0.0324$, $wR_2 = 0.0688$	$R_1 = 0.0463$, $wR_2 = 0.1075$
R indices (all data)	$R_1 = 0.0430$, $wR_2 = 0.0862$	$R_1 = 0.1100$, $wR_2 = 0.0850$	$R_1 = 0.0415$, $wR_2 = 0.0729$	$R_1 = 0.0810$, $wR_2 = 0.1240$
Largest difference in peak and hole ($e\ Å^{-3}$)	0.318 and −0.372	0.391 and −0.374	0.557 and −0.423	0.868 and −0.632

4.4. General procedure for ethylene oligomerization

Ethylene oligomerization at 1 atm of ethylene pressure was carried out as follows: the catalyst precursor was dissolved in toluene in a Schlenk tube and the reaction solution was stirred with a magnetic stir bar under ethylene atmosphere (1 atm) with the reaction temperature being controlled by water bath. Et_2AlCl and the solution of PPh_3 was added by a syringe. After a limited time, the reaction was terminated by acidified water, and the products were analyzed by GC.

Ethylene oligomerization at higher ethylene pressure was carried out in a 500 ml autoclave stainless steel reactor equipped with a mechanical stirrer and a temperature controller. Briefly, the catalyst precursor was dissolved in 50 ml toluene in a Schlenk tube and the desired amount of Et_2AlCl and PPh_3 was added. Then the mixture was immediately transferred into the reactor under ethylene atmosphere. Reaching the desired reaction temperature, ethylene with the desired pressure was introduced to start the reaction. After a limited time, the reaction was stopped. A small amount of the reaction solution was collected, terminated by the addition of 5% aqueous hydrogen chloride and then analyzed by gas chromatography (GC) for determining the distribution of oligomers obtained.

Acknowledgements

The project supported by NSFC No. 20473099. We thank Mr. Changxing Shao for English correction. K.W. was supported by DAAD postdoctoral fellowship.

Appendix A. Supplementary data

Supplementary data associated with this article can be found, in the online version, at doi:10.1016/j.jorganchem.2006.06.028.

References

[1] (a) S.D. Ittel, L.K. Johnson, M. Brookhart, Chem. Rev. 100 (2000) 1169;
(b) V.C. Gibson, S.K. Spitzmesser, Chem. Rev. 103 (2003) 283;
(c) F. Speiser, P. Braustein, L. Saussine, Acc. Chem. Res. 38 (2005) 784;
(d) S. Mecking, Angew. Chem. Int. Ed. 40 (2001) 534;
(e) W. Zhang, W. Zhang, W.-H. Sun, Prog. Chem. 17 (2005) 310;
(f) S. Jie, S. Zhang, W.-H. Sun, Petrochem. Tech. (Shiyou Huagong) 35 (2006) 297;
(g) W.-H. Sun, D. Zhang, S. Zhang, S. Jie, J. Hou, Kinet. Catal. 47 (2006) 278.

[2] (a) W. Keim, F.H. Kowaldt, R. Goddard, C. Krüger, Angew. Chem., Int. Ed. Engl. 17 (1978) 466;
(b) W. Keim, A. Behr, B. Limbäcker, C. Krüger, Angew. Chem., Int. Ed. Engl. 22 (1983) 503.

[3] L.K. Johnson, C.M. Killian, M. Brookhart, J. Am. Chem. Soc. 117 (1995) 6414.

[4] (a) B.L. Small, M. Brookhart, A.M.A. Bennett, J. Am. Chem. Soc. 120 (1998) 4049;
(b) G.J.P. Britovsek, V.C. Gibson, S.J. McTavish, G.A. Solan, A.J.P. White, D.J. Williams, B.S. Kimberley, P.J. Maddox, Chem. Commun. (1998) 849.

[5] (a) W. Keim, S. Killat, C.F. Nobile, G.P. Suranna, U. Englert, R. Wang, S. Mecking, D.L. Schröder, J. Organomet. Chem. 662 (2002) 150;
(b) W.-H. Sun, Z. Li, H. Hu, B. Wu, H. Yang, N. Zhu, X. Leng, H. Wang, New J. Chem. 26 (2002) 1474;
(c) F. Speiser, P. Braunstein, L. Saussine, R. Welter, Organometallics 23 (2004) 2613;
(d) F. Speiser, P. Braunstein, L. Saussine, Organometallics 23 (2004) 2625;
(e) F. Speiser, P. Braunstein, L. Saussine, Organometallics 23 (2004) 2633;
(f) F. Speiser, P. Braunstein, L. Saussine, Acc. Chem. Res. 38 (2005) 784.

[6] (a) W. Keim, Angew. Chem., Int. Ed. Engl. 29 (1990) 235;
(b) J. Heinicke, M. He, A. Dal, H.-F. Klein, O. Hetche, W. Keim, U. Flörke, H.-J. Haupt, Eur. J. Inorg. Chem. (2000) 431.

[7] (a) C.M. Killian, L.K. Johnson, M. Brookhart, Organometallics 16 (1997) 2005;
(b) S.A. Svejda, M. Brookhart, Organometallics 18 (1999) 65;
(c) S.P. Meneghetti, P.J. Lutz, J. Kress, Organometallics 18 (1999) 2734;
(d) T.V. Laine, K. Lappalainen, J. Liimatta, E. Aitola, B. Löfgren, M. Leskelä, Macromol. Rapid Commun. 20 (1999) 487;
(e) T.V. Laine, U. Piironen, K. Lappalainen, M. Klinga, E. Aitola, M. Leskelä, J. Organomet. Chem. 606 (2000) 112;
(f) B.Y. Lee, X. Bu, G.C. Bazan, Organometallics 20 (2001) 5425.

[8] (a) C. Wang, S. Friedrich, T.R. Younkin, R.T. Li, R.H. Grubbs, D.A. Bansleben, M.W. Day, Organometallics 17 (1998) 3149;
(b) C. Carlini, M. Isola, V. Liuzzo, A.M.R. Galletti, G. Sbrana, Appl. Catal. A: Gen. 231 (2002) 307;
(c) S. Wu, S. Lu, Appl. Catal. A: Gen. 246 (2003) 295;
(d) T.R. Younkin, E.F. Connor, J.I. Henderson, S.K. Friedrich, R.H. Grubbs, D.A. Bansleben, Science 287 (2000) 460;
(e) L. Wang, W.-H. Sun, L. Han, Z. Li, Y. Hu, C. He, C. Yan, J. Organomet. Chem. 650 (2002) 59;
(f) W.-H. Sun, W. Zhang, T. Gao, X. Tang, L. Chen, Y. Li, X. Jin, J. Organomet. Chem. 689 (2004) 917.

[9] X. Tang, W.-H. Sun, T. Gao, J. Hou, J. Chen, W. Chen, J. Organomet. Chem. 690 (2005) 1570.

[10] J. Hou, W.-H. Sun, S. Zhang, H. Ma, Y. Deng, X. Lu, Organometallics 25 (2006) 236.

[11] L. Wang, W.-H. Sun, L. Han, H. Yang, Y. Hu, X. Jin, J. Organomet. Chem. 658 (2002) 62.

[12] G.J.P. Britovsek, S.P.D. Baugh, O. Hoarau, V.C. Gibson, D.F. Wass, A.J.P. White, D.J. Williams, Inorg. Chim. Acta 345 (2003) 279.

[13] N. Ajellal, M.C.A. Kuhn, A.D.G. Boff, M. Hörner, C.M. Thomas, J.-F. Carpentier, O.L. Casagrande, Organometallics 25 (2006) 1213.

[14] W.-H. Sun, S. Jie, S. Zhang, W. Zhang, Y. Song, H. Ma, J. Chen, K. Wedeking, R. Fröhlich, Organometallics 25 (2006) 666.

[15] D.H. Camacho, E.V. Salo, J.W. Ziller, Z. Guan, Angew. Chem. Int. Ed. 43 (2004) 1821.

[16] J.C. Jenkins, M. Brookhart, Organometallics 22 (2003) 250.

[17] G.M. Sheldrick, SHELXTL-97, Program for the Refinement of Crystal Structures, University of Göttingen, Germany, 1997.